

Development 140, 3765–3776 (2013) doi:10.1242/dev.094961
 © 2013. Published by The Company of Biologists Ltd

Distinct temporal requirements for Runx1 in hematopoietic progenitors and stem cells

Joanna Tober, Amanda D. Yzaguirre, Eileen Piwarzyk and Nancy A. Speck*

SUMMARY

The transcription factor Runx1 is essential for the formation of yolk sac-derived erythroid/myeloid progenitors (EMPs) and hematopoietic stem cells (HSCs) from hemogenic endothelium during embryogenesis. However, long-term repopulating HSCs (LT-HSCs) persist when Runx1 is conditionally deleted in fetal liver cells, demonstrating that the requirement for Runx1 changes over time. To define more precisely when Runx1 transitions from an essential factor to a homeostatic regulator of EMPs and HSCs, and whether that transition requires fetal liver colonization, we performed conditional, timed deletions of Runx1 between E7.5 and E13.5. We determined that Runx1 loss reduces the formation or function of EMPs up through E10.5. The Runx1 requirement in HSCs ends later, as deletion up to E11.5 eliminates HSCs. At E11.5, there is an abrupt transition to Runx1 independence in at least a subset of HSCs that does not require fetal liver colonization. The transition to Runx1 independence in EMPs is not mediated by other core binding factors (Runx2 and/or Runx3); however, deleting the common non-DNA-binding β subunit (CBF β) severely compromises LT-HSC function. Hence, the requirements for Runx1 in EMP and HSC formation are temporally distinct, and LT-HSC function is highly reliant on continued core binding factor activity.

KEY WORDS: Runx1, Embryo, Hematopoiesis, Hemogenic endothelium, Mouse, Stem cells

INTRODUCTION

Hematopoiesis unfolds over a period of several days during murine embryogenesis (Dzierzak and Speck, 2008). The first progenitors arise in the yolk sac, initiating with primitive erythrocytes and megakaryocytes at embryonic stage (E) 7.25, followed by a second ‘wave’ of transient definitive erythroid/myeloid progenitors (EMPs) beginning at E8.25 (Palis et al., 1999; Tober et al., 2007). Lymphoid progenitors emerge autonomously in the yolk sac, para-aortic splanchnopleura (P-Sp) and placenta by E9.0 (Rhodes et al., 2008; Yoshimoto et al., 2011), and at E10.5 HSCs are detectable in the aorta/gonad/mesonephros (AGM) region and in vitelline and umbilical arteries (de Bruijn et al., 2000; Medvinsky and Dzierzak, 1996). At E11.5, HSCs capable of high level, multi-lineage engraftment can be found in all the aforementioned sites, and in the fetal liver (Dzierzak and Speck, 2008). At E12.5, the liver becomes the predominant hematopoietic organ in the fetus (Gekas et al., 2005; Kumaravelu et al., 2002).

EMPs, lymphoid progenitors and HSCs differentiate from hemogenic endothelium (Bertrand et al., 2010; Boisset et al., 2010; Chen et al., 2009; Kissa and Herbomel, 2010; Yoshimoto et al., 2011; Zovein et al., 2008). The conversion of hemogenic endothelium to blood occurs via an endothelial-to-hematopoietic cell transition, whereby endothelial cells with tight junctions round up, detach from the endothelial layer and enter the circulation. In many vertebrates, newly forming hematopoietic cells form clusters on the luminal side of the endothelial layer, which in mice express Kit (previously known as c-Kit) (Adamo and García-Cardena, 2012). Careful analysis of Kit⁺ cells in the major vasculature

documented their appearance starting at E9.0 [20 somite pairs (sp)] with total numbers of Kit⁺ cells and size of clusters peaking at E10.5 (33–34 sp) (Yokomizo and Dzierzak, 2010). A few Kit⁺ cells remain visible in the vasculature at E14.5. Lineage tracing of HSCs using a tamoxifen-activated Cre recombinase (Cre^{ERT}) expressed from the vascular endothelial cadherin (VEC; Cdh5 – Mouse Genome Informatics) regulatory sequences labeled 2–20% of adult bone marrow cells following tamoxifen injections at E9.5, and 4% when activated *ex vivo* at E11.5 (Zovein et al., 2008). Thus, EMP and HSC differentiation from hemogenic endothelium is a continuous, several day process extending from E8.25 through E11.5, and involves several different endothelial populations in distinct anatomical sites.

The formation of EMPs, lymphoid progenitors and HSCs from endothelium is strictly dependent on a heterodimeric transcription factor composed of a sequence specific DNA-binding protein, Runx1, and its obligate non-DNA-binding partner, core binding factor β (CBF β) (Chen et al., 2011; Chen et al., 2009). Deletion of Runx1 in endothelial cells with VEC-Cre blocked EMP and HSC formation, and the appearance of Kit⁺ hematopoietic cells in the vasculature (Chen et al., 2009). By contrast, conditional deletion of Runx1 in fetal liver cells using Vav1-Cre did not ablate either EMPs or HSCs, although downstream lineage-specific defects in lymphopoiesis and megakaryopoiesis were observed (Cai et al., 2011; Chen et al., 2009). Thus, hematopoiesis shifts from a Runx1-dependent to a relatively Runx1-independent state by the time EMPs and HSCs colonize the fetal liver.

It was not clear when during the period defined by the onset of VEC-Cre activity (E7.5) and onset of Vav1-Cre activity (E11.5–E13.5) (Chen et al., 2009) the transition from Runx1 dependence to independence occurred nor whether the transition to Runx1 independence required fetal liver colonization. Here, we determined precisely when the Runx1 requirement for EMP and HSC formation ends, by deleting Runx1 in a temporally controlled manner using tamoxifen-regulated Cre^{ERT} driven from either ubiquitously expressed or endothelial-specific transgenes. We show that the temporal requirement for Runx1 in EMP and HSC formation is

Abramson Family Cancer Research Institute and Department of Cell and Developmental Biology, Perelman School of Medicine, University of Pennsylvania, Philadelphia, PA 19104, USA.

* Author for correspondence (nancyas@exchange.upenn.edu)

Accepted 1 July 2013

distinct and the transition of HSCs to Runx1 independence does not require fetal liver colonization. Furthermore, we show that Runx2 and/or Runx3 do not mediate the transition to Runx1 independence in EMPs, whereas HSCs remain highly reliant on the activity of multiple core binding factors.

MATERIALS AND METHODS

Mice, timed breeding and staging

Transgenic mice expressing a tamoxifen-inducible Cre^{ERT} from the chicken β -actin promoter/enhancer coupled with the cytomegalovirus (CMV) immediate-early enhancer (B6.Cg-Tg[CAG-cre/Esr1]5Amc/J, s/n 004682) (Hayashi and McMahon, 2002) are from Jackson Laboratories. *Runx1* floxed mice (*Runx1^{tm3.1Spe}*) and *Runx1^{GFP}* mice (*Runx1^{tm4Dow}*) were previously described (Gowney et al., 2005; Lorsch et al., 2004). *Chfb* floxed mice (*Chfb^{tm1.1tan}*) were the kind gift of Ichiro Tanuichi (Naoe et al., 2007). *Cdh5*(PAC)-Cre^{ERT2} mice [Tg(Cdh5-cre/ERT2)1Rha] were provided by Ralf Adams (Sørensen et al., 2009) and *Vav1*-Cre mice [Tg(Vav1-cre)1Graf] by Thomas Graf (Stadtfeld and Graf, 2005).

Whole-mount immunohistochemistry and confocal microscopy

Embryos were prepared for confocal analysis as described (Yokomizo et al., 2012). The following primary antibodies were used: rat anti-mouse CD117 (clone 2B8, eBiosciences), rat anti-mouse CD31 (Mec 13.3, BD Pharmingen) and rabbit anti-human/mouse Runx1 (EPR3099, Epitomics, Burlingame, CA, USA). Secondary antibodies were purchased from Invitrogen: goat anti-rat Alexa Fluor 647, goat anti-rat Alexa Fluor 555 and goat anti-rabbit Alexa Fluor 488. Images were collected on a Zeiss LSM 710 confocal microscope equipped with 488-, 543- and 633-nm wavelengths and a 20 \times immersion objective (Plan-Apochromat 25 \times /0.8 NA). Data were acquired using Zeiss ZEN 2011 and processed using Fiji software (Schindelin et al., 2012), LOCI Bio-Formats Importer (<http://dev.loci.wisc.edu/fiji/>) and cell counter plugin (version 29 February 2008, Kurt De Vos; <http://rsb.info.nih.gov/ij/plugins/cell-counter.html>).

Tamoxifen injections of pregnant dams

Tamoxifen (MP Biomedicals) was prepared in 100% ethanol, diluted 1:10 in corn oil, and 2 mg per mouse administered by intraperitoneal injection.

Ex vivo whole embryo cultures

Whole embryo culture was performed as described by Takahashi et al. (Takahashi et al., 2008) with the following modifications. Intact embryos were cultured for 24 hours in 1 ml rat serum supplemented with 10 mM glucose and 10 μ M 4-hydroxytamoxifen (4-OHT, Sigma; prepared at 1000 \times in 95% ethanol) in a roller incubator (BTC Engineering, Cambridge, UK) at 37°C in 21% oxygen, 5% carbon dioxide and balanced nitrogen. Embryos that lacked a heartbeat, developed abnormally, or did not advance at least eight somite pairs were discarded. Tissues were washed in several changes of buffer to remove exogenous 4-OHT prior to hematopoietic culture.

Hematopoietic colony assay and PCR

CFU-C assays were performed in M3434 (StemCell Technologies, Vancouver, Canada) and scored at 1 week. Individual colonies were assayed by PCR. *Runx1* primers have been published previously (Chen et al., 2009). *Chfb* primers were: F3, 5'-GGTTAGGAGTCATTGTGATCAC-3'; R6, 5'-CATTGGATTGGCGTTACTGG-3'; R4, 5'-GAGGTACTTTTATTTT-GGAGTGAGG-3'.

qPCR

qPCR on FACS-sorted E10.5 hemogenic endothelium and clusters and E14.5 liver progenitors was performed using TaqMan Gene Expression Master Mix. *Cdh5* primers, (F: 5'-CAACTGCTCGTGAATCTCCA-3'; R: 5'-CGGTCAAGTATGGGAGTTT-3'), TaqMan probes (actb, 4352341E; HPRT, mm00-4469681-m1; Runx2, mm00501578-m1; Runx3, mm00490666-m1), and run on a 7900HT Fast Real-Time PCR machine (Applied Biosystems, South San Francisco, CA, USA).

Explant culture

AGM+U+V explant cultures were adapted from previously described methods (Medvinsky et al., 2008) using M5300 (StemCell Technologies)

supplemented with 10⁻⁶ M hydrocortisone hemisuccinate (Sigma) and 100 ng/ml each IL-3, SCF ligand, Flt3 ligand (PeproTech, Rocky Hill, NJ, USA) and 10 μ M 4-OHT (Sigma). PCR was performed on <5% of the cultured tissue to check that Runx1 deletion occurred in at least 50% of the cells.

Transplantation

Donor tissues from 129S1/SvImJ mice were transplanted into B6.SJL-Ptprca Pep3b/BoyJ recipients with 2.5 \times 10⁵ spleen cells (B6.SJL, Ly5.1/Ly5.2). E14.5 fetal liver was transplanted with 2.5 \times 10⁵ bone marrow competitor cells. Two split doses of 4.5-5 Gy were administered 3-4 hours apart from a Cs-137 source.

Flow cytometry

Flow cytometric analysis was performed on an LSR-II or sorting on a FACS Aria with DIVA software (Becton Dickinson, Franklin Lakes, NJ, USA) and data analyzed using FloJo (TreeStar, Ashland, OR, USA). The following monoclonal antibodies were used (from eBioscience and/or BD Biosciences): CD45.1-PE-cy7 (A20), CD45.2-PerCP-cy5.5 or CD45.2-FITC (104/A20), Gr1-FITC/PerCP-cy5.5/eFluor450 (RB6-8C5), Mac1-APC-cy7/eFluor 450 (M1/70), CD3e-PE/APC/eFluor 450 (145-2C11), CD19-PE/APC (1D3), Sca1-FITC or PerCP-cy5.5 (D7), c-Kit-APC-eFluor780 (2B8), CD135-PE (A2F10), CD34-APC (RAM34), CD48-APC (BCM1/HM481), Ter119-eFluor 450 (Ter-119) and B220-eFluor450 (RA3-6B2). CD150-PE-cy7 (TC15-12F12.2) was purchased from BioLegend. Red cells were lysed in Red Cell Lysis Buffer (Sigma). Dead cells were excluded using DAPI (Invitrogen). Population gates were set by comparison with fluor-minus-one controls.

RESULTS

Ubiquitous Runx1 deletion decreases erythroid/myeloid progenitors in the yolk sac, but not in the fetal liver

We deleted *Runx1* floxed (*Runx1^f*) alleles beginning at E7.5 in 24-hour windows using a ubiquitously expressed, tamoxifen-regulated Cre driven from the chicken β -actin promoter/enhancer coupled with the cytomegalovirus immediate-early enhancer (hereafter referred to as *Actb-Cre^{ERT}*) (Hayashi and McMahon, 2002). Runx1 was also specifically deleted in endothelial cells using Cre^{ERT} expressed from the VEC regulatory sequences (Sørensen et al., 2009). Embryos were either cultured *ex vivo* for 24 hours in the presence of the tamoxifen metabolite 4-hydroxytamoxifen (4-OHT) (Fig. 1A), or tamoxifen was injected into pregnant dams to execute the deletions (Fig. 1B). In both cases, embryos were harvested 24 hours post-tamoxifen exposure, exogenous tamoxifen was washed away, and hematopoiesis was analyzed.

We enumerated erythroid/myeloid progenitors in methylcellulose colony-forming assays. Prior to E10.0, the vast majority of erythroid/myeloid progenitors are yolk sac-derived EMPs (Lux et al., 2008). Afterwards, erythroid/myeloid progenitors include yolk sac-derived EMPs and progenitors that emerge autonomously in the AGM region, vitelline and umbilical arteries (AGM+U+V) and placenta. We refer to erythroid/myeloid progenitors in the yolk sac as 'EMPs', and those derived from other hematopoietic sites as colony forming units culture progenitors (CFU-Cs), recognizing that CFU-Cs could encompass progenitors (including EMPs) originating from multiple tissues.

We determined whether activation of Cre^{ERT} by tamoxifen or 4-OHT caused nonspecific toxicity by comparing the number of progenitors in *Runx1^{+/+}* and *Runx1^{f/f}* embryos in the presence or absence of *Actb-Cre^{ERT}*. Intraperitoneal injections of tamoxifen caused no significant reduction in the number of EMPs in the yolk sac or CFU-Cs in the AGM+U+V (Fig. 1D). However, there was a significant decrease in EMPs and CFU-Cs in whole embryos cultured in 4-OHT (Fig. 1C), which was accounted for in our data

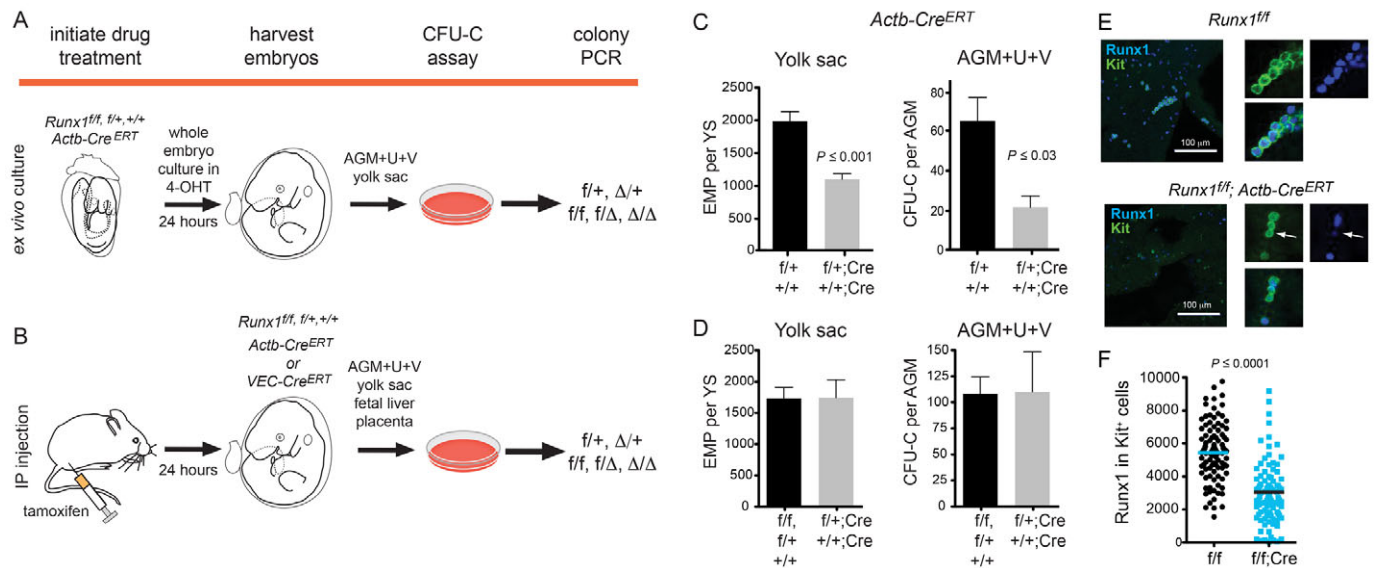


Fig. 1. Experimental strategy for deleting Runx1. (A) *Runx1* was deleted by culturing whole embryos *ex vivo* for 24 hours with 4-OHT. Embryos were staged prior to and at the end of the culture period. Hematopoietic tissues were washed, dissociated and plated in colony assays. Multiple individual colonies were analyzed by PCR for deletion of *Runx1^f* alleles. *f/+* and $\Delta/+$ represent colonies from a *Runx1^{f/+}; Cre^{ERT}* conceptus in which the *Runx1^f* allele was not deleted, or was deleted, respectively. *f/f*, *f/Δ* and Δ/Δ represent colonies from *Runx1^{f/f}; Cre^{ERT}* conceptuses in which no, one, or both *Runx1^f* alleles were deleted, respectively. (B) All deletions initiated at E9.5 onwards were performed by injecting pregnant dams with tamoxifen. Hematopoiesis was analyzed as shown in A. (C) The impact of Cre activation on progenitors following exposure to 4-OHT *ex vivo* in whole embryo cultures. Deletion was performed between E8.5 and E9.5. Genotypes of conceptuses are *Runx1^{f/+}* (*f/+*) and *Runx1^{f/+}* (*+/+*) (*n*=21), or *Runx1^{f/+}; Actb-Cre^{ERT}* (*f/+; Cre*) and *Runx1^{f/+}; Actb-Cre^{ERT}* (*+/+; Cre*) (*n*=8). (D) Progenitor numbers following tamoxifen injection of pregnant dams. Deletions were performed at E9.5 and embryos harvested at E10.5. All deletions were carried out with *Actb-Cre^{ERT}*. *+/+*, *f/+* and *f/f*, *n*=10 in yolk sac and *n*=8 in AGM+U+V. *+/+; Cre* and *f/+; Cre*, *n*=5 in yolk sac and *n*=6 in AGM+U+V. In C and D, error bars indicate s.e.m. (E) Whole-mount immunofluorescence of E10.5 yolk sacs harvested from dams injected with tamoxifen at E9.5, using antibodies recognizing endogenous Runx1 and Kit (maximum of 20 3-μm z-sections). Panels on the right are examples of Kit⁺ cells (green) with Runx1⁺ nuclei (blue). Arrows indicate a Kit⁺ cell with low Runx1 nuclear staining. Nuclear fluorescence intensity of Runx1 in individual Kit⁺ cells was quantified and plotted in panel F. (F) The average corrected nuclear fluorescence of Runx1 in 100 Kit⁺ cells.

interpretation. Runx1 protein decreased but did not entirely disappear in the majority of Kit⁺ cells in the yolk sac of *Runx1^{f/f}; Actb-Cre^{ERT}* embryos 24 hours post-tamoxifen injection (Fig. 1E,F). However, Runx1 protein decreased below a critical threshold because, as shown in Fig. 2, *Runx1^{f/f}; Actb-Cre^{ERT}* yolk sacs had significantly decreased EMP numbers when deletion was induced at specific developmental times.

We compared the number of EMPs in *Runx1^{f/f}; Cre^{ERT}* embryos with *Runx1^{f/+}; Cre^{ERT}* embryos to control for potential Cre^{ERT} toxicity for deletions performed in whole embryo cultures (Fig. 2). We note that the comparison with *Runx1^{f/+}; Cre^{ERT}* embryos could underestimate the impact of *Runx1* deletion because *Runx1* haploinsufficiency negatively impacts EMP numbers (Wang et al., 1996). EMP numbers in *Runx1^{f/f}* and *Runx1^{f/+}* yolk sacs (without Cre^{ERT}) peaked at E9.5–E10.0, as shown previously (Palis et al., 1999), then gradually declined over the following two days (Fig. 2A; see also supplementary material Table S1). Deletion of *Runx1^{f/f}* by *Actb-Cre^{ERT}* (*f/f; Cre*) in 24-hour windows up to E10.5 significantly decreased EMPs in the yolk sac compared with *Runx1^{f/+}; Actb-Cre^{ERT}* controls (*f/+; Cre*); thus, Runx1 deletion negatively impacted EMP formation and/or function over a 3-day period.

We assessed deletion of the *Runx1* alleles in individual EMP-derived colonies from *Runx1^{f/+}; Actb-Cre^{ERT}* and *Runx1^{f/f}; Actb-Cre^{ERT}* yolk sacs by PCR (Fig. 2B,C; supplementary material Table S2). There were no colonies from *Runx1^{f/f}; Actb-Cre^{ERT}* yolk sacs containing two deleted *Runx1* alleles (Δ/Δ) at E8.5 (deletion initiated at E7.5), but colonies with two deleted *Runx1* alleles were

detected at all later time points. A colony with two deleted *Runx1* alleles indicates that the EMP from which it differentiated was no longer Runx1 dependent at the time of deletion. Despite detecting colonies with two deleted *Runx1* alleles as early as E9.0, the significant decline in EMP numbers indicates that a subset of EMPs or their hemogenic endothelial precursors remained Runx1 dependent up through E10.5.

We examined the effect of Runx1 deletion on CFU-Cs in the AGM+U+V (Fig. 2A). However, the overall number of CFU-Cs in the AGM+U+V is low compared with that of EMPs in the yolk sac, indicating that many of the AGM+U+V CFU-Cs are likely to be circulating yolk sac-derived EMPs (Lux et al., 2008). Although there was a significant decrease in AGM+U+V CFU-Cs at E11.5, the extent to which that reflects a decrease in yolk sac-derived EMPs or AGM+U+V-derived CFU-Cs cannot be determined.

Deletion of *Runx1* caused only modest reductions in CFU-Cs in the fetal liver (Fig. 2A), and at all times there were colonies containing two deleted *Runx1* alleles in *Runx1^{f/f}; Actb-Cre^{ERT}* fetuses (Fig. 2C). Therefore, once CFU-Cs reach the fetal liver they are no longer Runx1 dependent, supporting previous data obtained using *Vav1-Cre* (Chen et al., 2009).

Runx1 is continuously required in hemogenic endothelium for EMP formation

To examine the requirement for Runx1 in hemogenic endothelium we used *VEC-Cre^{ERT}*. VEC-Cre^{ERT} deletion occurs in endothelium, but the extent to which it continues to delete in newly forming

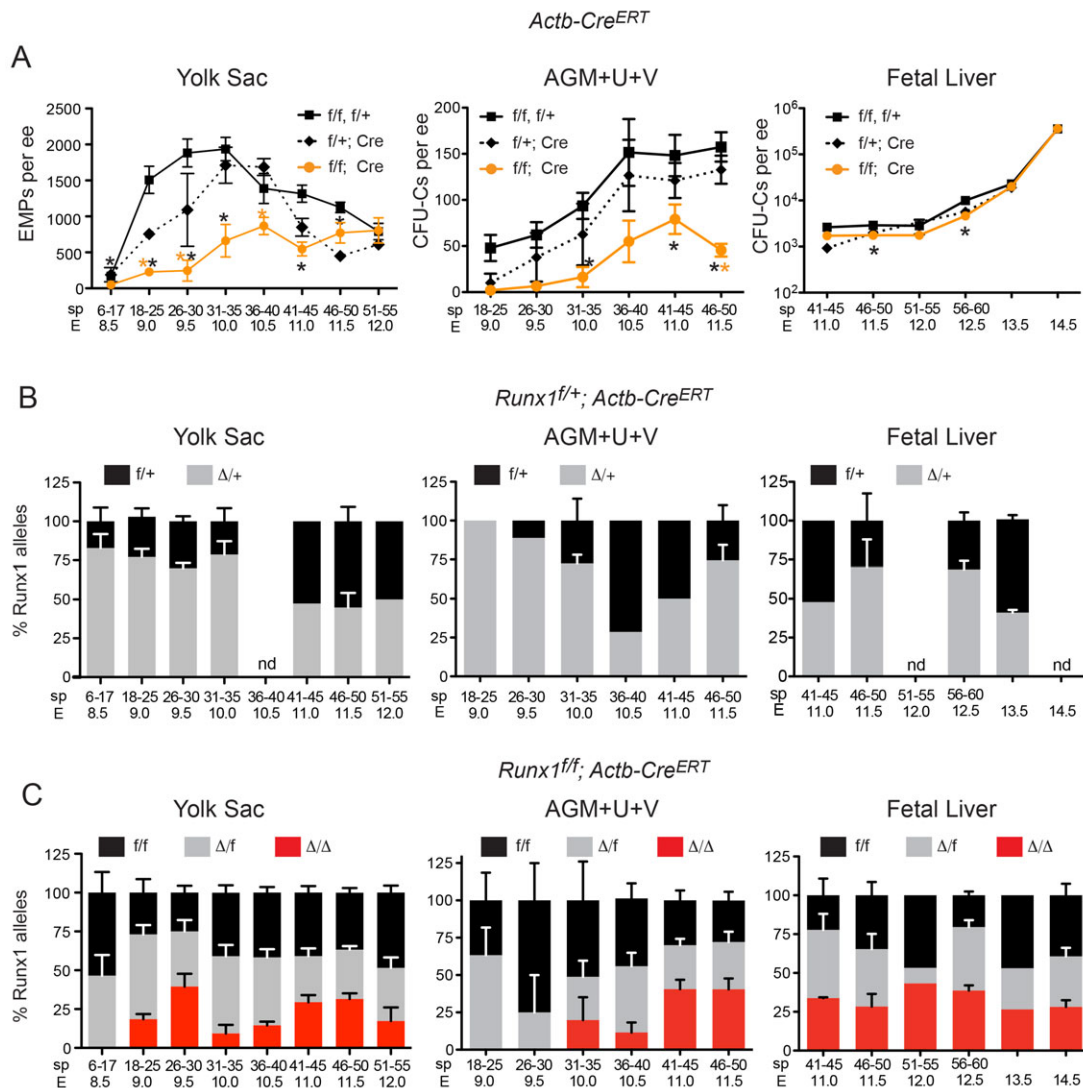


Fig. 2. Deletion of Runx1 decreases EMPs in the yolk sac, but not CFU-Cs in the fetal liver. (A) Yolk sac EMPs, AGM+U+V CFU-Cs and fetal liver CFU-Cs [mean±s.e.m. per embryonic equivalent (ee)] following deletion of *Runx1* with *Actb-Cre^{ERT}*. Embryonic ages in somite pairs (sp) and embryonic days (E) on the x-axis represent the stage of the embryo when harvested for methylcellulose colony assays, with the deletion initiated 24 hours earlier. Black asterisks indicate significant differences ($P \leq 0.05$) between colony numbers in *f/f*; Cre versus *f/f* and *f/+* embryos. Orange asterisks indicate significant differences between *f/f*; Cre and *f/+*; Cre embryos. The difference between *f/f*; Cre and *f/+*; Cre at 18–25 sp (E9.0) in yolk sac is statistically significant ($P = 0.06$). (B) Deletion frequency in *Runx1^{f/+}; Actb-Cre^{ERT}* yolk sac, AGM+U+V, and fetal liver EMPs/CFU-Cs represented as percentages of colonies (mean±s.e.m.) that had no deletion (*f/+*) or deletion ($\Delta/+$) of the floxed allele. The average deletion efficiency in combined experiments was 64.7% (± 4.04). Data from embryos in which the average deletion frequency was <30% were excluded from Fig. 2A. (C) Deletion frequency in *Runx1^{f/f}; Actb-Cre^{ERT}* progenitors represented as percentages of colonies (average±s.e.m.) that had deleted both (Δ/Δ), one (Δ/f) or no *Runx1^f* alleles (*f/f*). The average deletion efficiency was 61.4% (± 19.1). The number of sample replicates and colonies are shown in supplementary material Tables S1, S2. All data were analyzed using Student's unpaired *t*-test and are shown as mean±s.e.m.

hematopoietic clusters is unknown. Deletion by VEC-Cre^{ERT} from E10.0 to E11.0 in *Runx1^{f/f}; VEC-Cre^{ERT}* fetuses had no effect on fetal liver CFU-C numbers (Fig. 3A) and the efficiency of deletion in *Runx1^{f/f}; VEC-Cre^{ERT}* fetal liver CFU-Cs was only 7.5% (Fig. 3B); thus, VEC-Cre^{ERT} appeared to be minimally active in fully formed fetal liver CFU-Cs. These data are consistent with a previous study reporting low deletion frequency in fetal liver blood cells, presumably because VEC-Cre^{ERT} levels and activity have substantially declined (Zovein et al., 2008). It is possible that VEC-Cre^{ERT} activity declines even before cells reach the fetal liver because in the chicken embryo, VEC (*Cdh5*) mRNA is downregulated in intra-arterial clusters

(Jaffredo et al., 2005). To determine whether this also occurs in mouse, we sorted GFP⁺ cells from the AGM+U+V of E10.5 embryos expressing GFP from a functional *Runx1* allele (Lorsbach et al., 2004), separated the cells into fractions containing hemogenic endothelium [*Runx1* (GFP)⁺ VEC⁺ CD45⁺ (Ptpcr)⁺] and hematopoietic clusters [*Runx1* (GFP)⁺ VEC⁺ CD45⁺], and analyzed the expression of VEC by qPCR (Fig. 3C). VEC mRNA levels were sixfold lower in clusters compared with hemogenic endothelium, confirming that VEC expression is also downregulated in clusters in the mouse. Nevertheless, residual VEC-Cre^{ERT} activity in cluster cells cannot be ruled out.

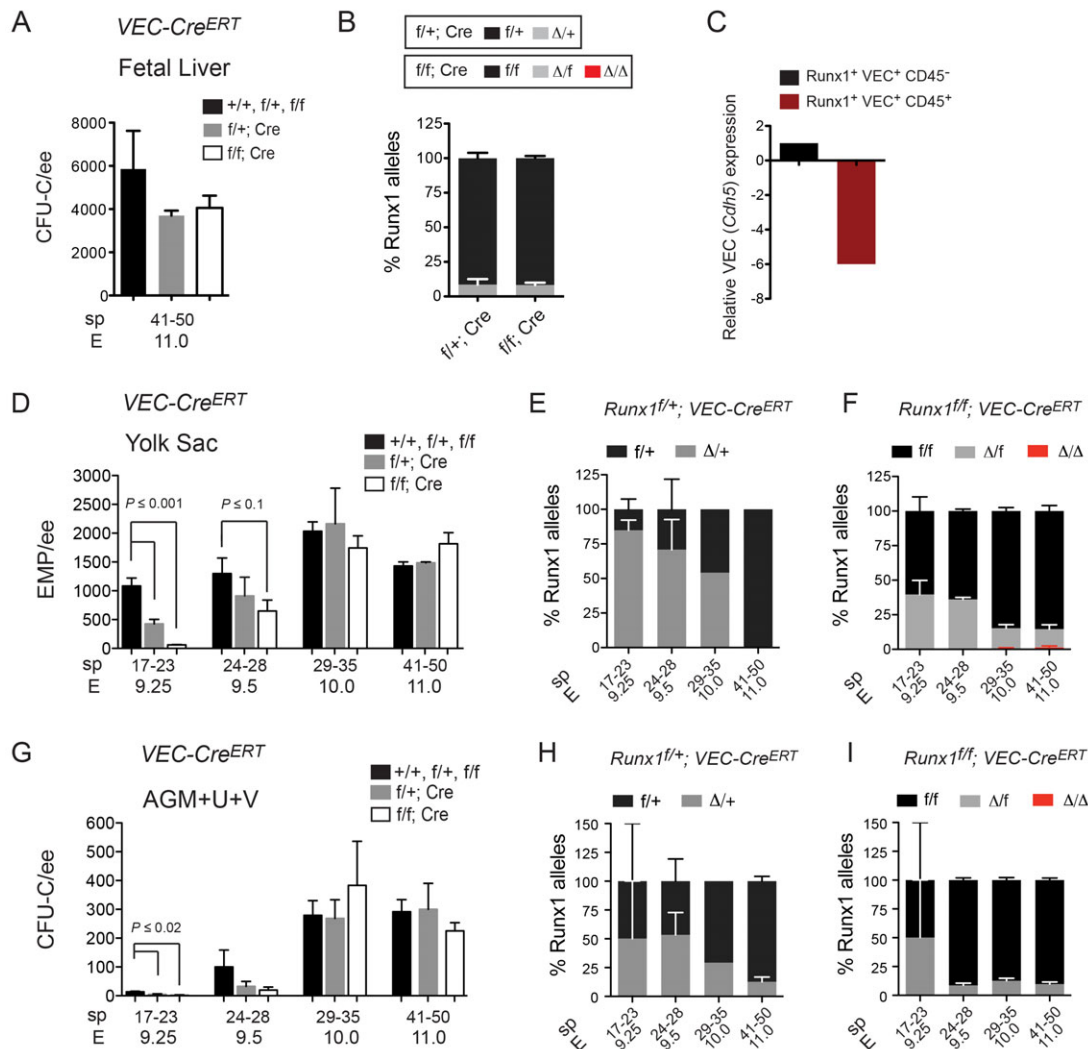


Fig. 3. Runx1 is required in VEC-Cre^{ERT}-expressing cells at all times. (A) Number of CFU-Cs (mean±s.e.m.) in fetal livers of various *Runx1* genotypes with and without VEC-Cre^{ERT}, following injection of tamoxifen into pregnant dams at E10.0 and isolation of fetuses at E11.0. (B) Deletion frequency in fetal liver CFU-Cs by VEC-Cre^{ERT} represented as percentages of colonies (mean±s.e.m.) with no (f/+ or f/f), one (Δ/+ or Δ/f) or two (Δ/Δ) deleted *Runx1* alleles. (C) Expression of VEC (*Cdh5*) mRNA in E10.5 AGM+U+V from sorted Runx1 (GFP⁺) VEC⁺ CD45⁺ hematopoietic cells relative to Runx1 (GFP⁺) VEC⁺ CD45⁻ endothelial cells (represented as fold change). (D) Number of yolk EMPs (mean±s.e.m.) following deletion of Runx1 with VEC-Cre^{ERT}. All deletions were performed by tamoxifen injection of pregnant dams. (E) Deletion frequency in *Runx1*^{f/+}; VEC-Cre^{ERT} yolk sac EMPs (mean±s.e.m.). (F) Deletion frequency in *Runx1*^{f/f}; VEC-Cre^{ERT} yolk sac EMPs. (G) Number of AGM+U+V CFU-Cs (mean±s.e.m.) following deletion of Runx1 with VEC-Cre^{ERT}. (H) Deletion frequency in *Runx1*^{f/+}; VEC-Cre^{ERT} AGM+U+V CFU-Cs represented as percentages of colonies (mean±s.e.m.) that had not deleted (f/+) or deleted (Δ/+) the floxed *Runx1* allele. (I) Deletion frequencies in *Runx1*^{f/f}; VEC-Cre^{ERT} AGM+U+V CFU-Cs. The number of sample replicates and colonies assayed are shown in supplementary material Tables S3, S4. Student's unpaired t-tests were performed on data shown in A,B,D-I.

The frequency of deleted *Runx1* alleles was high (70-80%) in yolk sac EMPs from 17-23 sp and 24-28 sp embryos (Fig. 3E,F; supplementary material Table S4), indicating that many EMPs are forming from hemogenic endothelium (or to be more precise, VEC-Cre^{ERT}-expressing cells) at those times. Additionally, EMP numbers were significantly decreased in 17-23 sp *Runx1*^{f/f}; VEC-Cre^{ERT} yolk sacs, and there was a trend towards decreased numbers in 24-28 sp yolk sacs (Fig. 3D; supplementary material Table S3). Older (41-50 sp) embryos showed much lower deletion efficiency in EMPs (Fig. 3E,F), and EMP numbers were not decreased (Fig. 3D). Thus, by E11.0, most yolk sac EMPs had completed their differentiation from hemogenic endothelium. The frequency at which both *Runx1* alleles were deleted in the yolk sac of *Runx1*^{f/f}; VEC-Cre^{ERT}

embryos was very low (3 out of 427 colonies) (Fig. 3F), indicating that although the number of EMPs differentiating from hemogenic endothelium decreases with time, Runx1 is required in hemogenic endothelium (or in VEC-Cre^{ERT}-expressing cells) at all times.

The effects of Runx1 deletion by VEC-Cre^{ERT} on AGM+U+V CFU-Cs followed the same trend as observed in yolk sac EMPs (Fig. 3G-I), with interpretation subject to the same caveats described for Actb-Cre^{ERT}.

Runx1 is essential for HSC formation up to E11.5

To determine when Runx1 is essential for HSC formation, we injected pregnant dams with tamoxifen at E9.5 or E10.5, isolated the AGM+U+V from E11.5 embryos, explanted the tissues for 3

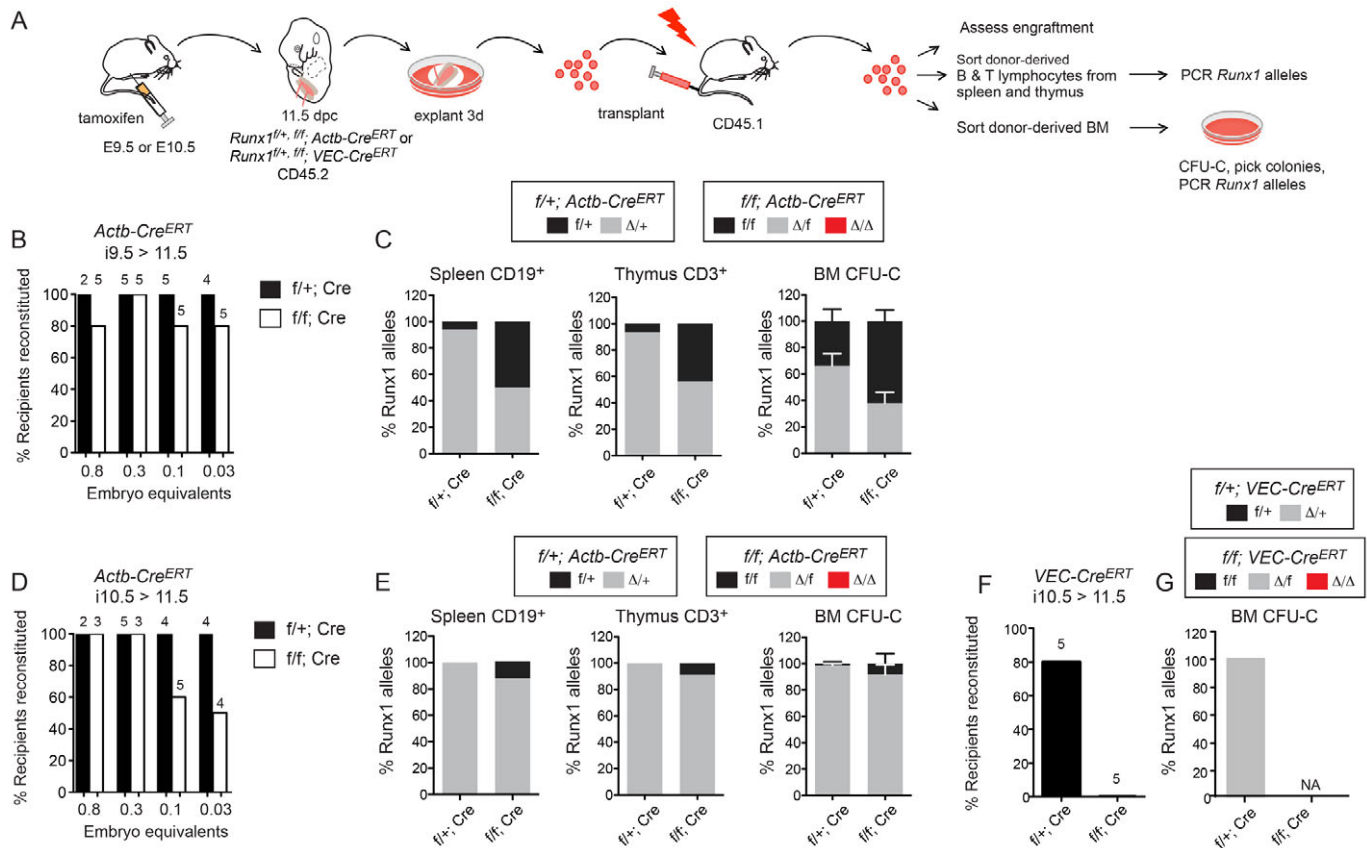


Fig. 4. Runx1 is essential for pre-HSC/HSC formation in the AGM prior to E11.5. (A) Experimental strategy for deletion in pre-HSCs/HSCs. Pregnant dams were injected with tamoxifen at E9.5 or E10.5. AGM+U+V were harvested at E11.5 and explanted in the absence of tamoxifen for 3 days prior to transplantation into irradiated hosts. Recipients were analyzed for engraftment, then donor-derived (CD45.2⁺) cells were FACS sorted 16-weeks post-transplantation and directly analyzed by PCR (splenic B cells and thymic T cells) or cultured in methylcellulose (bone marrow) and colonies were assayed by PCR. (B) Percentage of transplant recipients reconstituted with >1% donor Mac-1⁺ bone marrow cells at 16 weeks. Pregnant dams were injected with tamoxifen at E9.5 (i9.5), and AGM+U+V harvested at E11.5. The number of animals transplanted is indicated above the bars. The percentage contribution at the lowest dose at which all recipients were reconstituted [0.3 embryo equivalents (ee)] by *Runx1*^{f/f}; *Actb-Cre*^{ERT} HSCs ranged from 96.4% to 99.6% (mean=97.8%), and by *Runx1*^{f/f}; *Actb-Cre*^{ERT} HSCs from 87.6% to 99.0% (mean=94.2%). All recipients reconstituted with Mac-1⁺ cells contained donor-derived B and T cells. (C) Percentage of deleted *Runx1* alleles from sorted donor-derived CD45.2⁺ cells (injections at E9.5), from transplants shown in B (*Actb-Cre*^{ERT}). Deletion data in the spleen and thymus represent intensity of PCR products from 40,000 cells. Deletion data in individual CD45.2 bone marrow colonies (BM CFU-C) were averaged from all recipients (±s.e.m.). *Runx1*^{f/f}; *Actb-Cre*^{ERT}=266 colonies and *Runx1*^{f/f}; *Actb-Cre*^{ERT}=340 colonies. (D) Percentage of transplant recipients reconstituted with >1% donor Mac-1⁺ bone marrow cells at 16 weeks when tamoxifen was injected into pregnant dams at E10.5, analyzed as in B. The percentage contribution at 0.3 embryo equivalents by *Runx1*^{f/f}; *Actb-Cre*^{ERT} HSCs ranged from 84.2% to 99.8% (mean=95.9%), and by *Runx1*^{f/f}; *Actb-Cre*^{ERT} HSCs from 24.2% to 79.6% (mean=56.5%). All recipients reconstituted with Mac-1⁺ cells contained donor-derived B and T cells. (E) Percentage of deleted *Runx1* alleles from sorted donor-derived CD45.2⁺ cells for injections carried out at E10.5, analyzed as in C. The number of colonies analyzed by PCR was 73 for donor-derived (CD45.2) *Runx1*^{f/f}; *Actb-Cre*^{ERT} BM CFU-Cs and 168 for *Runx1*^{f/f}; *Actb-Cre*^{ERT} BM CFU-Cs. (F) Percentage of transplant recipients reconstituted with >1% donor Mac-1⁺ bone marrow cells at 16 weeks when tamoxifen was injected into pregnant dams at E10.5 (deletion with *VEC-Cre*^{ERT}). The number of animals transplanted is indicated above the bars. All recipients were transplanted with 0.16 ee of donor cells. The percentage contribution by *Runx1*^{f/f}; *VEC-Cre*^{ERT} HSCs ranged from 85% to 92.9% (mean=89.4%). (G) Percentage of deleted *Runx1* alleles from sorted donor-derived CD45.2⁺ cells for injections carried out at E10.5, analyzed as in C and E. Eighty-six colonies were analyzed by PCR for *Runx1*^{f/f}; *VEC-Cre*^{ERT} donor-derived BM CFU-Cs. NA, no colonies analyzed (because *Runx1*^{f/f}; *VEC-Cre*^{ERT} cells did not reconstitute).

days to expand the HSCs, and transplanted the cells into irradiated adult mice (Fig. 4A). A freshly isolated E11.5 AGM contains only one HSC, but it contains many pre-HSCs that can be matured into HSCs by incorporating a several day explant culture step prior to transplantation (Kumaravelu et al., 2002; Taoudi et al., 2008). Thus, robust engraftment is possible even if pre-HSC/HSC numbers are moderately lowered by deletion. Injection of as few as 0.03 embryo equivalents (ee) of explanted AGM+U+V from E11.5 *Runx1*^{f/f}; *Actb-Cre*^{ERT} fetuses isolated from dams injected with tamoxifen at E9.5 resulted in long-term, high level, multi-lineage engraftment of all recipient mice; thus, each explanted AGM region contained at

least 30 HSCs (Fig. 4B). Identically treated cells from *Runx1*^{f/f}; *Actb-Cre*^{ERT} fetuses provided similar levels of engraftment in the majority of recipient mice (Fig. 4B).

We determined whether mice transplanted with *Runx1*^{f/f}; *Actb-Cre*^{ERT} cells were engrafted with HSCs with both *Runx1* alleles deleted, which would indicate that Runx1 was not required in pre-HSCs/HSCs at the time of deletion. Conversely, if recipients were repopulated exclusively by HSCs containing only one or no deleted *Runx1* alleles, this would reveal that Runx1 was essential in pre-HSCs/HSCs at the time of deletion. Donor-derived thymic CD3⁺ T cells, splenic CD19⁺ B cells, and donor cells from the bone marrow

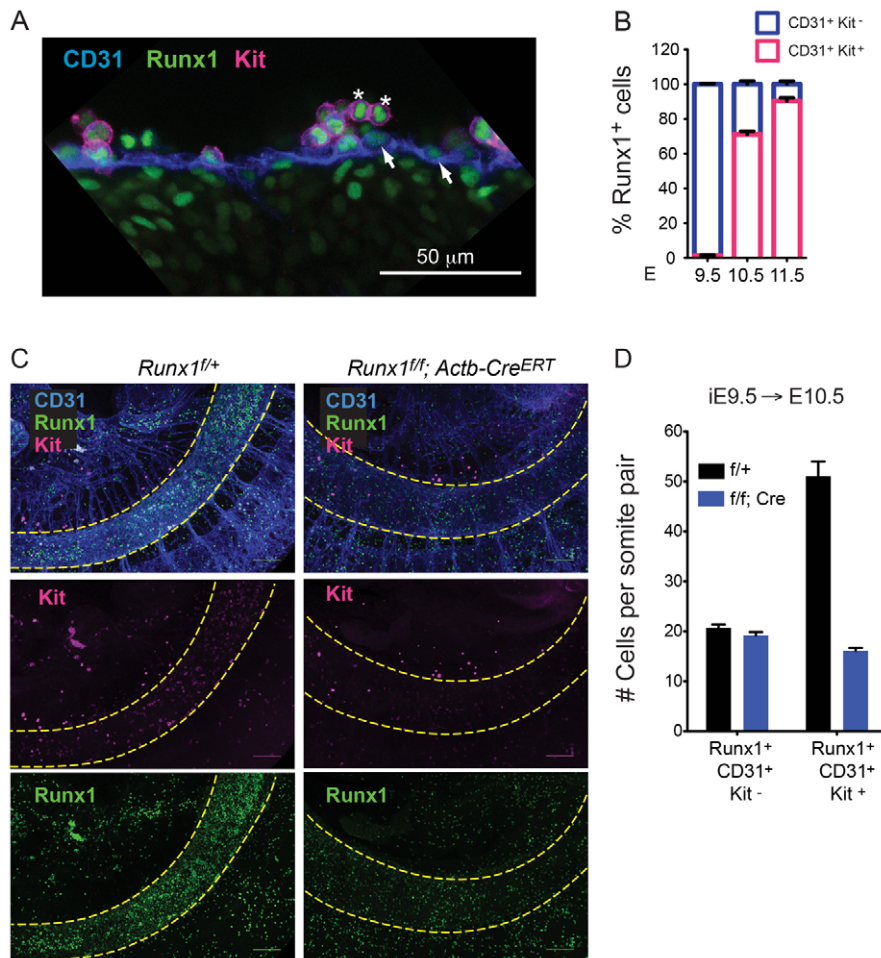


Fig. 5. Deletion of Runx1 reduces the number of hematopoietic clusters in the dorsal aorta. (A) Whole-mount confocal microscopy of Runx1⁺ CD31⁺ endothelial cells (examples with arrows) and Runx1⁺ CD31⁺ Kit⁺ hematopoietic cluster cells (examples with asterisks) in the dorsal aorta. Image is a sum of three 2- μ m z-sections. (B) Fraction of Runx1⁺ cells (average \pm s.e.m.) distributed between the endothelium (CD31⁺ Kit⁻) and hematopoietic clusters (CD31⁺ Kit⁺) of the dorsal aorta at three stages (two embryos per stage). (C) Whole-mount immunofluorescence of E10.5 embryos following tamoxifen injection of pregnant dams at E9.5 (iE9.5). Each image is a 365- μ m deep z-stack composite with the dorsal aorta outlined in yellow. (D) Average number (\pm s.d.) ($n=2$) of Runx1⁺ cells per somite pair in the dorsal aorta.

of recipient mice were isolated and analyzed for the status of *Runx1* alleles. *Runx1* deletion efficiency in donor T or B cells derived from *Runx1*^{f/+}; *Actb-Cre*^{ERT} HSCs was very high (>90%) and the *Runx1*^f allele was deleted in >60% of individual donor-derived colonies from the bone marrow (Fig. 4C). However, no donor-derived cells from *Runx1*^{f/f}; *Actb-Cre*^{ERT} HSCs contained two deleted *Runx1* alleles, indicating that there was exquisitely strong selection for retaining at least one functional *Runx1* allele between E9.5-E11.5 in pre-HSCs/HSCs.

We next determined whether Runx1 was required from E10.5-E11.5 for pre-HSC/HSC formation (Fig. 4D). The deletion efficiency in donor-derived B cells, T cells and CFU-C progenitors from *Runx1*^{f/+}; *Actb-Cre*^{ERT} HSCs was very high (99-100%; Fig. 4E). Despite the extremely high deletion efficiency, we found no donor-derived cells from *Runx1*^{f/f}; *Actb-Cre*^{ERT} HSCs containing two deleted *Runx1* alleles (Fig. 4E), indicating that Runx1 is absolutely required for pre-HSC/HSC formation or function in the AGM+U+V between E9.5 and E11.5.

We then investigated whether Runx1 was required in hemogenic endothelial (VEC-Cre^{ERT}-expressing) cells from E9.5 to E11.5. Strikingly, no recipients were reconstituted when Runx1 was deleted from E9.5 to E11.5 (not shown) or from E10.5 to E11.5 (Fig. 4F). The frequency of deletion was 100% in donor-derived *Runx1*^{f/+}; *VEC-Cre*^{ERT} CFU-Cs (Fig. 4G). Therefore, Runx1 is essential in VEC-Cre^{ERT}-expressing cells for pre-HSC/HSC formation between E10.5 and E11.5. Furthermore, all pre-HSCs/HSCs present between E10.5 and E11.5 express VEC-Cre^{ERT}.

To quantify the conversion of Runx1⁺ hemogenic endothelial cells into clusters over the time points analyzed, we examined the distribution of Runx1⁺ cells between the endothelium and Kit⁺ clusters in the dorsal aorta of E9.5, E10.5 and E11.5 wild-type embryos. Almost all Runx1⁺ cells were endothelial at E9.5, only 30% remained in the endothelium at E10.5, and 10% were endothelial at E11.5 (Fig. 5A,B). Therefore, the major conversion of Runx1⁺ hemogenic endothelium to cluster cells occurs between E9.5 and E10.5, coinciding with when cluster cell numbers peak (Yokomizo and Dzierzak, 2010). *Runx1* deletion between E9.5 and E10.5 decreased the number of cluster cells (Fig. 5C,D). However, all functional pre-HSCs/HSCs are still lost when Runx1 is deleted with VEC-Cre^{ERT} one day later, between E10.5 and E11.5. Thus, Runx1 is still required in at least a subset of pre-HSCs/HSCs after most hemogenic endothelial cells have already differentiated into cluster cells. As it is unknown whether VEC-Cre^{ERT} is active only in endothelial cells, or if it is also active in all or a subset of cluster cells, Runx1 could be required in the hemogenic endothelium, the cluster cells, or both.

At least a subset of HSCs have transitioned to Runx1 independence at E11.5

To determine whether Runx1 was required in pre-HSCs/HSCs after E11.5, we cultured E11.5 AGM+U+V as explants in the presence of 4-OHT for 3 days, dissociated the explants, washed to remove drug, then transplanted the cells into irradiated hosts (Fig. 6A). All recipients of *Runx1*^{f/+}; *Actb-Cre*^{ERT} AGM+U+V had

high level, multi-lineage engraftment, whereas only four out of seven recipients of *Runx1^{f/f}; Actb-Cre^{ERT}* AGM+U+V were engrafted (Fig. 6B). Although the fraction of recipients engrafted by *Runx1^{f/f}; Actb-Cre^{ERT}* HSCs was lower, they were repopulated by *Runx1*-deficient HSCs as ~90% of colonies picked from methylcellulose cultures of donor-derived bone marrow cells had two deleted *Runx1* alleles (Fig. 6C). The reduced engraftment by *Runx1*-deficient HSCs is consistent with the observation that *Runx1*-deficient LT-HSCs are slightly impaired. For example, the fetal liver and bone marrow of *Runx1^{f/f}; Vav1-Cre* animals have threefold fewer functional LT-HSCs (Cai et al., 2011). *Runx1*-deficient LT-HSCs also contribute less efficiently than do wild-type LT-HSCs to differentiated cells in peripheral blood (Cai et

al., 2011; Gowney et al., 2005; Ichikawa et al., 2004). However, we conclude that, despite reduced engraftment, *Runx1* is not essential for the maturation and/or expansion of at least a subset of pre-HSCs/HSCs starting at E11.5 in the AGM+U+V.

We then determined whether *Runx1* was required in *VEC-Cre^{ERT}*-expressing cells for pre-HSC/HSC formation after E11.5 using the same strategy. There was no difference in the fraction of engrafted recipient mice transplanted with *Runx1^{f/+}; VEC-Cre^{ERT}* or *Runx1^{f/f}; VEC-Cre^{ERT}* cells (Fig. 6D), unlike what was observed with *Actb-Cre^{ERT}* deletion (Fig. 6B). The frequency of deletion in *Runx1^{f/+}; VEC-Cre^{ERT}* donor-derived CFU-C progenitors was 100% (Fig. 6E), indicating that *VEC-Cre^{ERT}* was active in the vast majority of pre-HSCs/HSCs at E11.5. However, and in striking

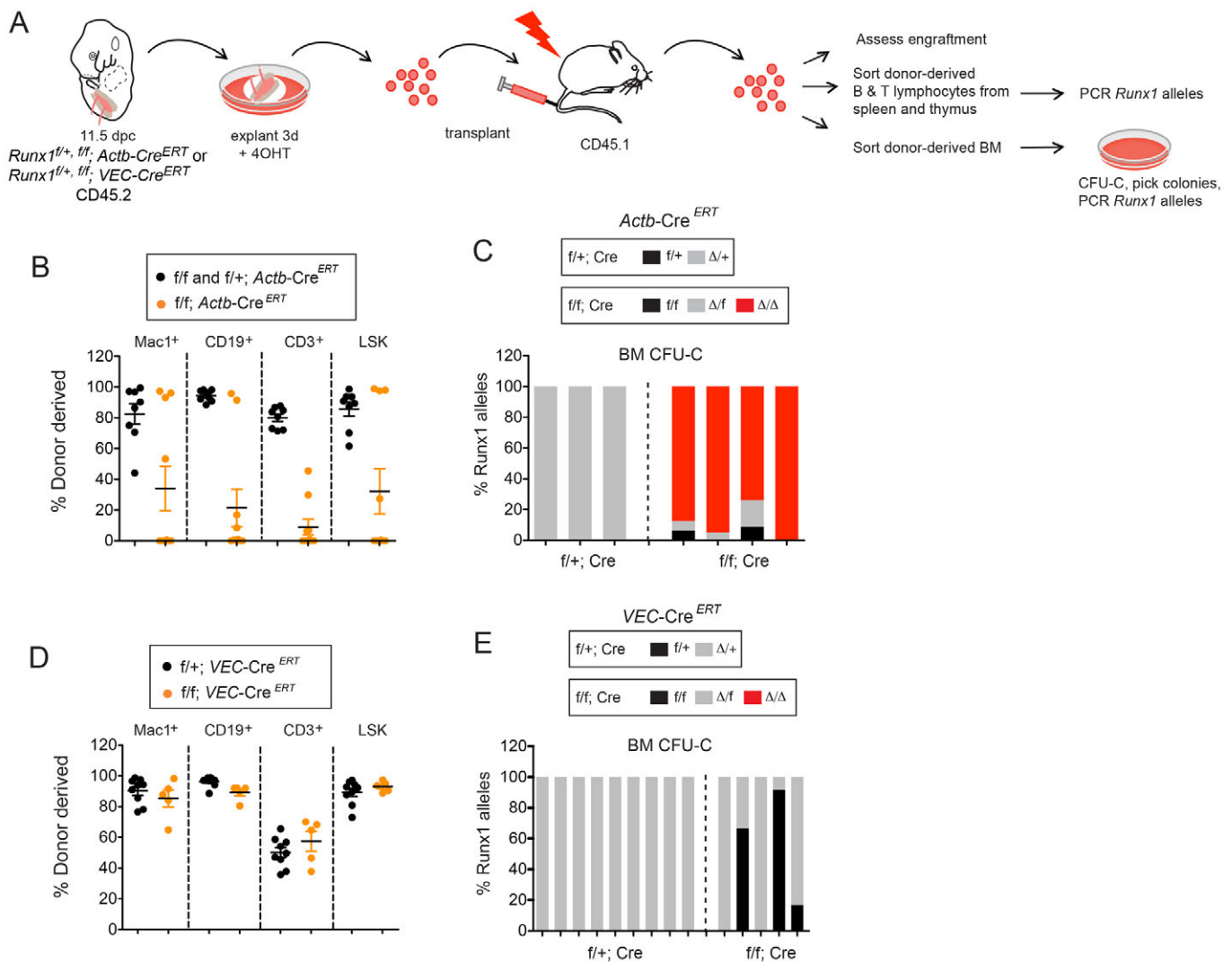


Fig. 6. *Runx1* is required for HSC maturation prior to E11.5 in the AGM+U+V. (A) Schematic for deletion of *Runx1* *ex vivo*. E11.5 AGM+U+V (CD45.2⁺) were explanted in 4-OHT for three days, dissociated, and transplanted into irradiated CD45.1⁺ hosts with 250,000 CD45.1/CD45.2 spleen cells. Recipients were analyzed 16 weeks post-transplantation, and CD45.2⁺ donor cells (mean±s.e.m.) sorted from bone marrow and thymus of reconstituted recipients and analyzed for *Runx1* deletion by PCR, as described in Fig. 4. (B) Percentage of donor-derived cells in the bone marrow 16 weeks post-transplantation following deletion with *Actb-Cre^{ERT}*. Contribution to peripheral blood was similar to bone marrow (not shown). Embryonic equivalents of 1.0 and 1.6 were transplanted. (C) PCR analysis of *Runx1* alleles from *Actb-Cre^{ERT}* donor-derived colonies picked from methylcellulose cultures. Number of colonies assayed=31 for *f/+*; *Actb-Cre^{ERT}* and 137 for *f/f*; *Actb-Cre^{ERT}*. Each bar represents colonies from an independent recipient mouse. (D) Percentage of donor-derived cells (mean±s.e.m.) in the bone marrow 16 weeks post-transplantation following deletion with *VEC-Cre^{ERT}*. Contribution to peripheral blood was similar to bone marrow (not shown). Embryonic equivalent of 0.2 was transplanted. (E) PCR analysis of *Runx1* alleles from *VEC-Cre^{ERT}* deleted donor-derived colonies picked from methylcellulose cultures from individual recipients. Number of colonies assayed=106 for *f/+*; *VEC-Cre^{ERT}* and 60 for *f/f*; *VEC-Cre^{ERT}*. Each bar represents colonies from an independent recipient mouse.

contrast to the data obtained with Actb-Cre^{ERT}, no recipients were engrafted with *Runx1*^{fl/fl}; *VEC-Cre*^{ERT} HSCs in which both *Runx1* alleles were deleted (Fig. 6E). Therefore, pre-HSCs/HSCs in which either one or two *Runx1*^{fl} alleles escaped deletion by VEC-Cre^{ERT}, and therefore retained Runx1 function, had matured/expanded to sufficient numbers in the explant cultures to repopulate 100% of the recipients.

Together, these data show that Runx1 is essential for pre-HSC/HSC formation in the AGM region prior to E11.5, at which time some HSCs transition to Runx1 independence. Runx1 remains essential in cells that express VEC-Cre^{ERT}.

The transition to Runx1 independence is an epigenetic event

Runx1 is one of three DNA-binding subunits in the core binding factor family. One potential mechanism for the transition to Runx1

independence might be that Runx2 and/or Runx3 compensates for Runx1 loss. To address this possibility, we inactivated all three Runx proteins by deleting *Cbfb*, the gene encoding their common non-DNA-binding subunit, using *Vav1-Cre*. *Cbfb*^{fl/fl}; *Vav1-Cre* fetal livers at E14.5 had increased numbers of CFU-Cs (Fig. 7A), similar to what was observed upon deletion of *Runx1* with *Vav1-Cre* (Chen et al., 2009). There was no upregulation of either Runx2 or Runx3 in E14.5 fetal liver progenitors (Lineage⁻ Kit⁺ cells) by qPCR (not shown), and therefore increased Runx2 and/or Runx3 levels are unlikely to be compensating for Runx1 loss. Thus, Runx1 is the only important Runx subunit in CFU-Cs, and the transition to Runx1 independence is unlikely to be due to functional redundancy with Runx2 and/or Runx3.

There were no significant reductions in phenotypic HSC populations in the E14.5 fetal liver of *Cbfb*^{fl/fl}; *Vav1-Cre* animals, including long-term repopulating HSCs [LT-HSCs, CD48⁻ CD150

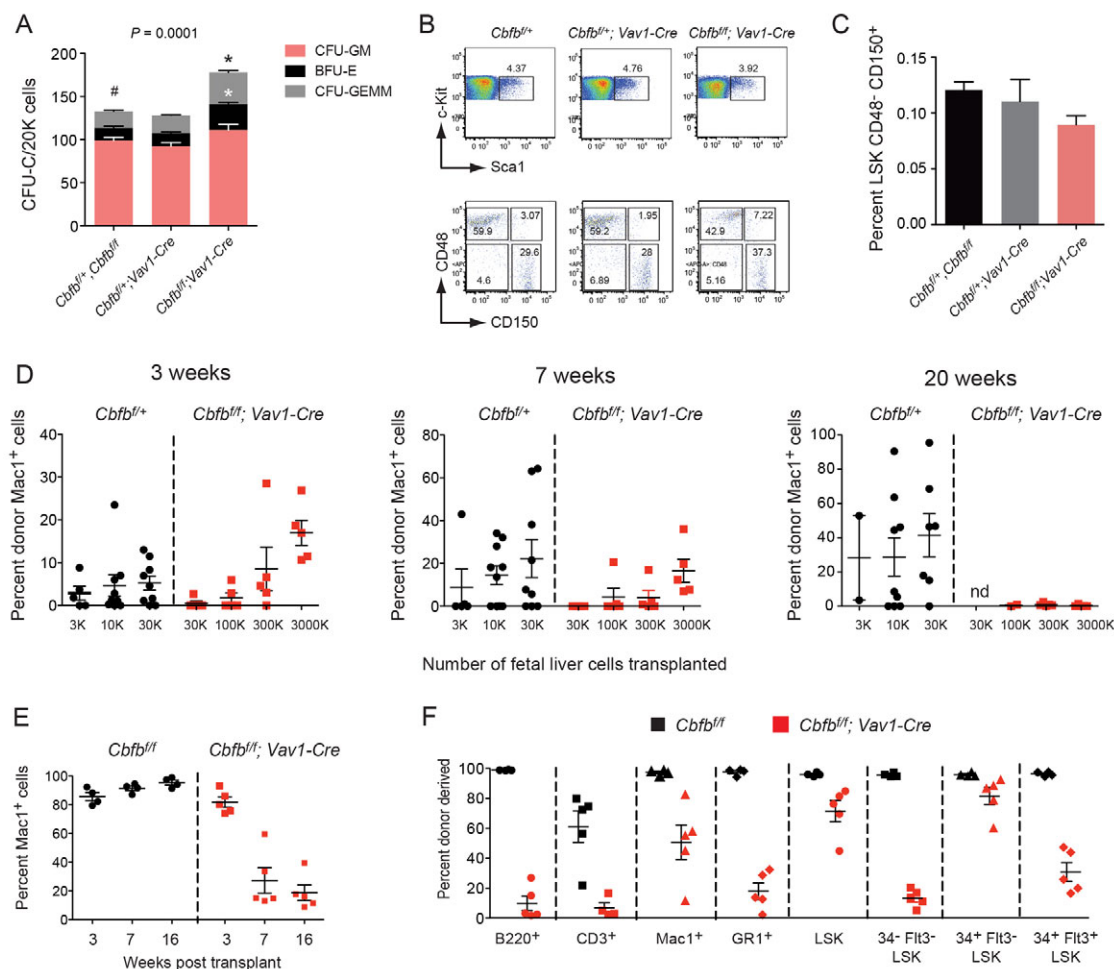


Fig. 7. Runx2 and Runx3 do not compensate for Runx1 loss in fetal liver CFU-Cs. (A) CFU-Cs (\pm s.e.m.) per 20,000 E14.5 fetal liver cells from *Cbfb*^{fl/fl} and *Cbfb*^{fl/fl}; *Vav1-Cre* ($n=6$), *Cbfb*^{fl/fl}; *Vav1-Cre* ($n=4$), and *Cbfb*^{fl/fl}; *Vav1-Cre* fetuses ($n=7$). Significance was determined by one-way ANOVA. Asterisk indicates a significant difference compared with controls (#) determined by Dunnett's Multiple Comparison test. (B) Representative flow cytometry profiles of LSK and other phenotypic HSC populations using SLAM markers (CD48, CD150) in E14.5 fetal livers. (C) Percentage (mean \pm s.e.m.) of phenotypic LT-HSCs in E14.5 fetal livers. *Cbfb*^{fl/fl}, *Cbfb*^{fl/fl}; *Vav1-Cre*, $n=5$. *Cbfb*^{fl/fl}; *Vav1-Cre*, $n=4$. (D) Competitive transplant of various numbers of *Cbfb*^{fl/fl} and *Cbfb*^{fl/fl}; *Vav1-Cre* E14.5 fetal liver cells. Plotted are the percentages (mean \pm s.e.m.) of CD45.2 donor-derived Mac1⁺ cells in the peripheral blood at 3, 7 and 20 weeks post-transplant. Each dot represents an individual transplant recipient. CD45.1/CD45.2 bone marrow cells (2×10^5) were used as competitors. (E) Noncompetitive transplant of 2×10^6 E14.5 fetal liver cells. Contribution to Mac1⁺ cells in peripheral blood is plotted (mean \pm s.e.m.). (F) Contribution of donor-derived cells to various populations in the bone marrow of recipients transplanted with 2×10^6 E14.5 fetal liver cells (mean \pm s.e.m.). The contribution of *Cbfb*^{fl/fl}; *Vav1-Cre* cells to all populations was significantly lower than that of *Cbfb*^{fl/fl} cells, with the exception of short-term (ST)-HSCs (CD34⁺ Flt3⁻ LSK).

(Slamf1)⁺ Ter119⁻ Gr1⁻ CD3e⁻ B220⁻ Sca1⁺ Kit⁺ (LSK)] (Fig. 7B,C). To determine whether functional LT-HSCs were present, we transplanted several doses of E14.5 *Chfb*^{f/f}; *Vav1-Cre* fetal liver cells along with 2×10⁵ adult bone marrow competitors, and measured donor contribution to Mac-1 (Itgam)⁺ cells in peripheral blood. *Chfb*^{f/f}; *Vav1-Cre* fetal liver cells could provide short-term (3 weeks) contribution to Mac-1⁺ cells in at least a subset of recipients at all doses tested (Fig. 7D). However, no donor contribution was evident at 20 weeks post-transplant at any dose. This was not caused by a block in differentiation, as there was no accumulation of stem and progenitor cells in the marrow, except in one recipient (not shown). We also assessed engraftment following transplantation of a large number of fetal liver cells (2×10⁶) in a non-competitive setting. This resulted in transient high-level contribution to peripheral blood at 3 weeks, followed by a decline in donor-derived cells that leveled off to ~18% at 16 weeks with replacement by residual host cells (Fig. 7E). The bone marrow contained donor-derived LSK cells consisting primarily of CD34⁺ Flt3⁻ LSK cells (phenotypic short-term HSCs) and, to a lesser extent, multipotent progenitor cells (MPPs) (CD34⁺ Flt3⁺ LSK) and Mac-1⁺ cells (Fig. 7F). Contribution to phenotypic LT-HSCs (CD34⁺ Flt3⁻ LSK), B220⁺ B cells and CD3⁺ T cells in the bone marrow was much lower. The one recipient containing sufficient numbers of donor-derived CD3⁺ thymocytes to analyze was repopulated with T cells that contained only one deleted *Chfb* allele, indicating strong selection for retaining a functional *Chfb* allele in T cells (data not shown). However, both *Chfb* alleles were deleted in donor-derived B cells sorted from the spleens of this and all other transplant recipients, and in all of 57 colonies isolated from methylcellulose in which donor-derived bone marrow was plated (data not shown); therefore, recipients were engrafted with CBFβ-deficient LT-HSCs. We conclude that, although severely compromised when directly transplanted, and completely outcompeted in a competitive setting, LT-HSCs are present in the fetal livers of *Chfb*^{f/f}; *Vav1-Cre* mice. Nevertheless, CBFβ-deficient HSCs are much more severely compromised than Runx1-deficient HSCs (Cai et al., 2011), and therefore Runx2 and/or Runx3 contribute substantially to LT-HSC function.

DISCUSSION

Runx1 is required in hemogenic endothelium for EMP and HSC formation, but once EMPs and HSCs colonize the fetal liver they are Runx1 independent (Chen et al., 2009). Runx1 is expressed in yolk sac mesoderm or hemogenic endothelium over a several day period spanning E7.5 to sometime after E11.5, and whether Runx1 was required for that entire period or a discrete window within it was not known. Here, we show that Runx1 is continuously required in hemogenic endothelium (or in VEC-Cre^{ERT}-expressing cells) for both EMP and HSC formation, as deletion with VEC-Cre^{ERT} at any time resulted in essentially no EMPs or no HSCs with two deleted *Runx1* alleles. Nevertheless, the times at which deletion of Runx1 most significantly affected EMP versus HSC formation were distinct, and reflected when the majority of EMPs and HSCs differentiate from hemogenic endothelium. Most EMPs have differentiated from hemogenic endothelium by E10.5, and *Runx1* deletion up until that time, but not afterwards, negatively impacted EMP numbers. Conversely, deletion of Runx1 between E10.5 and E11.5 had no impact on EMP numbers, yet completely eliminated HSCs and pre-HSCs in the AGM plus umbilical and vitelline arteries. The separate temporal requirements for Runx1 for EMP versus HSC formation is consistent with the fact that EMPs and HSCs are first detected at different times (Dzierzak and Speck,

2008). These data are in accord with our previous demonstration of distinct temporal requirements for CBFβ in EMP versus HSC formation (Chen et al., 2011).

Tanaka et al. (Tanaka et al., 2012) previously showed that restoration of Runx1 expression from the endogenous *Runx1* locus at E6.5 and E7.5 could rescue EMP formation and viability of Runx1-deficient embryos, whereas restoring Runx1 expression at E8.0 or later could not. Their experimental design utilized Cre^{ERT} expressed from one endogenous *Runx1* allele to permanently restore Runx1 expression from the other, conditionally activated *Runx1* allele. The Tanaka et al. (Tanaka et al., 2012) study defines the beginning of the Runx1 requirement for EMP formation as E7.5, and we have defined the end of the requirement as E10.5. The end of the requirement is likely to reflect the termination of a three-day process of EMP formation from endothelium. Tanaka et al. also defined the beginning of the Runx1 requirement for HSC formation as E7.5 (Tanaka et al., 2012). Although they showed by transplantation experiments that HSCs were rescued when Runx1 was reactivated at E7.5, they did not directly assess HSC function by transplantation upon reactivation at later time points, and instead used fetal viability and CFU-C activity in the AGM region as surrogates for HSC rescue. However, HSCs can form in the AGM region in the absence of CFU-C activity or fetal viability (Chen et al., 2011); thus, these are not reliable surrogates for HSCs. Thus, the earliest time at which Runx1 function must be present for HSC formation remains ambiguous. Here, we established that Runx1 is absolutely required from E10.5 to E11.5 in the AGM+U+V for pre-HSCs/HSCs that can be expanded or matured in explant cultures, but starting at E11.5, some pre-HSCs/HSCs have transitioned to Runx1 independence. Our data do not preclude the possibility that some Runx1-independent pre-HSCs/HSCs emerged prior to E10.5 and had already colonized the fetal liver, as our assessment of pre-HSCs/HSCs was restricted to the AGM+U+V. The transition to Runx1 independence does not require the fetal liver microenvironment, as it can occur in AGM+U+V explant cultures, and appears to be a temporally controlled event.

It was suggested that the transition of EMPs to Runx1 independence could be mediated by the onset of Runx2 and/or Runx3 expression, which could then compensate for Runx1 loss (Hoogenkamp et al., 2009). However, we demonstrated that deletion of *Chfb* with *Vav1-Cre*, which would affect the activity of all three Runx proteins, was permissive for EMP/CFU-C function. It is more likely that Runx1 establishes a chromatin state in hemogenic endothelium and EMPs, and at some point is no longer required to maintain this state. A global analysis of Runx1 binding in embryonic stem cell (ESC)-derived hemogenic endothelial cells confirms the first tenant of this hypothesis (Lichtinger et al., 2012). Using endothelium derived from Runx1-deficient ESCs containing a doxycycline-inducible form of Runx1, Lichtinger et al. (Lichtinger et al., 2012) showed that Runx1 functioned as a pioneer factor that could bind to chromatin at sites distant from promoters with low or negligible levels of the activating H3K9 acetylation mark, and strongly induce acetylation. The transcription factors Tal1 and Fli1, which are expressed in hemogenic endothelium, bound hematopoietic-specific genes in the absence of Runx1, but Runx1 induction led to a rapid redistribution of these factors to sites in the vicinity of Runx1-occupied sites. The mechanism underlying the transition from unstable to stable epigenetic states no longer requiring Runx1 is a fascinating question, and is probably a multistep process involving cooperation with different chromatin regulatory proteins, or with direct or indirect transcription factor targets of Runx1.

The E10.5 mouse embryo contains ~800 Kit⁺ cells in hematopoietic clusters in the dorsal aorta, but almost no functional HSCs (Müller et al., 1994; Yokomizo and Dzierzak, 2010). However, the E10.5 AGM region contains pre-HSCs that can be matured into HSCs during a 3-5 day explant culture period. Rybtsov et al. (Rybtsov et al., 2011) showed that all pre-HSCs in the E10.5 AGM region were in the VEC⁺ CD45⁻ population, which contains endothelial cells and a subset of cells in the clusters, and none was in the VEC⁺ CD45⁺ cluster population. We showed that deletion of *Runx1* with VEC-Cre^{ERT} between E10.5 and E11.5, followed by explant culture, eliminated all HSCs. This indicates that all pre-HSCs in the AGM+U+V between E10.5 and E11.5 still express VEC-Cre^{ERT} and require Runx1. The VEC-Cre^{ERT}-expressing cells include hemogenic endothelium, but might also include some or all cells within clusters, as VEC-Cre^{ERT} deletion could potentially occur in cluster cells. Beginning at E11.5, pre-HSCs appear that are Runx1 independent. Deletion at E11.5 with Actb-Cre^{ERT} results in HSCs with two deleted *Runx1* alleles, but at no time will deletion with VEC-Cre^{ERT} allow the emergence of Runx1-deficient HSCs. Therefore, Runx1 is always required in a VEC-Cre^{ERT}-expressing cell for pre-HSC/HSC formation, regardless of the developmental time.

Finally, our observation that CBFβ-deficient LT-HSCs are severely impaired sheds light on an interesting observation in leukemia. Although bi-allelic loss-of-function mutations in *RUNX1* have been observed by multiple investigators in acute myelogenous leukemia, bi-allelic mutations in *CBFB* have not been reported (Mangan and Speck, 2011). It may be that loss of all core binding factor activity is incompatible with maintaining a leukemic or pre-leukemic stem cell, and they are easily outcompeted by normal HSCs. Therefore, drugs that target CBFβ and interfere with its ability to interact with Runx proteins could potentially have clinical utility if a therapeutic window in which activity in leukemic or pre-leukemic stem cells, but not in normal HSCs can be identified.

Acknowledgements

We thank Ichiro Taniuchi for the *Cbfb* floxed mice; Ralf Adams for the VEC-Cre^{ERT} mice; Lucio Castilla for the *Cbfb* primer sequences; and Nate Levin for technical help.

Funding

This work was supported by grants from the National Institutes of Health (NIH) [R01HL091724 (to N.A.S.), T32CA09140 (to J.T. and A.D.Y.) and U01HL100504 (to E.P.)]. J.T. is further supported by the Leukemia and Lymphoma Society [3217-12]. Core services were supported by the Abramson Family Cancer Research Institute and the Abramson Cancer Center. Deposited in PMC for release after 12 months.

Competing interests statement

The authors declare no competing financial interests.

Author contributions

J.T. performed all of the experiments with the following exceptions: A.D.Y. contributed to the whole-mount immunohistochemistry, confocal microscopy and related data analysis; E.P. performed the qRT-PCR and related data analysis in Fig. 4C. N.A.S. contributed to the intellectual and experimental design, data analysis and manuscript preparation.

Supplementary material

Supplementary material available online at <http://dev.biologists.org/lookup/suppl/doi:10.1242/dev.094961/-/DC1>

References

- Adamo, L. and García-Cardena, G. (2012). The vascular origin of hematopoietic cells. *Dev. Biol.* **362**, 1-10.
- Bertrand, J. Y., Chi, N. C., Santoso, B., Teng, S., Stainier, D. Y. and Traver, D. (2010). Haematopoietic stem cells derive directly from aortic endothelium during development. *Nature* **464**, 108-111.

- Boisset, J. C., van Cappellen, W., Andrieu-Soler, C., Galjart, N., Dzierzak, E. and Robin, C. (2010). In vivo imaging of haematopoietic cells emerging from the mouse aortic endothelium. *Nature* **464**, 116-120.
- Cai, X., Gaudet, J. J., Mangan, J. K., Chen, M. J., De Obaldia, M. E., Oo, Z., Ernst, P. and Speck, N. A. (2011). Runx1 loss minimally impacts long-term hematopoietic stem cells. *PLoS ONE* **6**, e28430.
- Chen, M. J., Yokomizo, T., Zeigler, B. M., Dzierzak, E. and Speck, N. A. (2009). Runx1 is required for the endothelial to haematopoietic cell transition but not thereafter. *Nature* **457**, 887-891.
- Chen, M. J., Li, Y., De Obaldia, M. E., Yang, Q., Yzaguirre, A. D., Yamada-Inagawa, T., Vink, C. S., Bhandoola, A., Dzierzak, E. and Speck, N. A. (2011). Erythroid/myeloid progenitors and hematopoietic stem cells originate from distinct populations of endothelial cells. *Cell Stem Cell* **9**, 541-552.
- de Bruijn, M. F., Speck, N. A., Peeters, M. C. and Dzierzak, E. (2000). Definitive hematopoietic stem cells first develop within the major arterial regions of the mouse embryo. *EMBO J.* **19**, 2465-2474.
- Dzierzak, E. and Speck, N. A. (2008). Of lineage and legacy: the development of mammalian hematopoietic stem cells. *Nat. Immunol.* **9**, 129-136.
- Gekas, C., Dieterlen-Lièvre, F., Orkin, S. H. and Mikkola, H. K. (2005). The placenta is a niche for hematopoietic stem cells. *Dev. Cell* **8**, 365-375.
- Gronney, J. D., Shigematsu, H., Li, Z., Lee, B. H., Adelsperger, J., Rowan, R., Curley, D. P., Kutok, J. L., Akashi, K., Williams, I. R. et al. (2005). Loss of Runx1 perturbs adult hematopoiesis and is associated with a myeloproliferative phenotype. *Blood* **106**, 494-504.
- Hayashi, S. and McMahon, A. P. (2002). Efficient recombination in diverse tissues by a tamoxifen-inducible form of Cre: a tool for temporally regulated gene activation/inactivation in the mouse. *Dev. Biol.* **244**, 305-318.
- Hoogenkamp, M., Lichtinger, M., Krysinska, H., Lancrin, C., Clarke, D., Williamson, A., Mazzearella, L., Ingram, R., Jorgensen, H., Fisher, A. et al. (2009). Early chromatin unfolding by RUNX1: a molecular explanation for differential requirements during specification versus maintenance of the hematopoietic gene expression program. *Blood* **114**, 299-309.
- Ichikawa, M., Asai, T., Saito, T., Seo, S., Yamazaki, I., Yamagata, T., Mitani, K., Chiba, S., Ogawa, S., Kurokawa, M. et al. (2004). AML-1 is required for megakaryocytic maturation and lymphocytic differentiation, but not for maintenance of hematopoietic stem cells in adult hematopoiesis. *Nat. Med.* **10**, 299-304.
- Jaffredo, T., Bollerot, K., Sugiyama, D., Gautier, R. and Drevon, C. (2005). Tracing the hemangioblast during embryogenesis: developmental relationships between endothelial and hematopoietic cells. *Int. J. Dev. Biol.* **49**, 269-277.
- Kissa, K. and Herbomel, P. (2010). Blood stem cells emerge from aortic endothelium by a novel type of cell transition. *Nature* **464**, 112-115.
- Kumaravelu, P., Hook, L., Morrison, A. M., Ure, J., Zhao, S., Zuyev, S., Ansell, J. and Medvinsky, A. (2002). Quantitative developmental anatomy of definitive haematopoietic stem cells/long-term repopulating units (HSC/RUs): role of the aorta-gonad-mesonephros (AGM) region and the yolk sac in colonisation of the mouse embryonic liver. *Development* **129**, 4891-4899.
- Lichtinger, M., Ingram, R., Hannah, R., Müller, D., Clarke, D., Assi, S. A., Lie-A-Ling, M., Noailles, L., Vijayabaskar, M. S., Wu, M. et al. (2012). RUNX1 reshapes the epigenetic landscape at the onset of haematopoiesis. *EMBO J.* **31**, 4318-4333.
- Lorsbach, R. B., Moore, J., Ang, S. O., Sun, W., Lenny, N. and Downing, J. R. (2004). Role of RUNX1 in adult hematopoiesis: analysis of RUNX1-IRES-GFP knock-in mice reveals differential lineage expression. *Blood* **103**, 2522-2529.
- Lux, C. T., Yoshimoto, M., McGrath, K., Conway, S. J., Palis, J. and Yoder, M. C. (2008). All primitive and definitive hematopoietic progenitor cells emerging before E10 in the mouse embryo are products of the yolk sac. *Blood* **111**, 3435-3438.
- Mangan, J. K. and Speck, N. A. (2011). RUNX1 mutations in clonal myeloid disorders: from conventional cytogenetics to next generation sequencing, a story 40 years in the making. *Crit. Rev. Oncog.* **16**, 77-91.
- Medvinsky, A. and Dzierzak, E. (1996). Definitive hematopoiesis is autonomously initiated by the AGM region. *Cell* **86**, 897-906.
- Medvinsky, A., Taoudi, S., Mendes, S. and Dzierzak, E. (2008). Analysis and manipulation of hematopoietic progenitor and stem cells from murine embryonic tissues. *Curr. Protoc. Stem Cell Biol.* **4**:2A.6.1-2A.6.25.
- Müller, A. M., Medvinsky, A., Strouboulis, J., Grosveld, F. and Dzierzak, E. (1994). Development of hematopoietic stem cell activity in the mouse embryo. *Immunity* **1**, 291-301.
- Naoy, Y., Setoguchi, R., Akiyama, K., Muroi, S., Kuroda, M., Hatam, F., Littman, D. R. and Taniuchi, I. (2007). Repression of interleukin-4 in T helper type 1 cells by Runx/Cbf beta binding to the Il4 silencer. *J. Exp. Med.* **204**, 1749-1755.
- Palis, J., Robertson, S., Kennedy, M., Wall, C. and Keller, G. (1999). Development of erythroid and myeloid progenitors in the yolk sac and embryo proper of the mouse. *Development* **126**, 5073-5084.
- Rhodes, K. E., Gekas, C., Wang, Y., Lux, C. T., Francis, C. S., Chan, D. N., Conway, S., Orkin, S. H., Yoder, M. C. and Mikkola, H. K. (2008). The

- emergence of hematopoietic stem cells is initiated in the placental vasculature in the absence of circulation. *Cell Stem Cell* **2**, 252-263.
- Rybtsov, S., Sobiesiak, M., Taoudi, S., Souilhol, C., Senserrich, J., Liakhovitskaia, A., Ivanovs, A., Frampton, J., Zhao, S. and Medvinsky, A. (2011). Hierarchical organization and early hematopoietic specification of the developing HSC lineage in the AGM region. *J. Exp. Med.* **208**, 1305-1315.
- Schindelin, J., Arganda-Carreras, I., Frise, E., Kaynig, V., Longair, M., Pietzsch, T., Preibisch, S., Rueden, C., Saalfeld, S., Schmid, B. et al. (2012). Fiji: an open-source platform for biological-image analysis. *Nat. Methods* **9**, 676-682.
- Sörensen, I., Adams, R. H. and Gossler, A. (2009). DLL1-mediated Notch activation regulates endothelial identity in mouse fetal arteries. *Blood* **113**, 5680-5688.
- Stadtfield, M. and Graf, T. (2005). Assessing the role of hematopoietic plasticity for endothelial and hepatocyte development by non-invasive lineage tracing. *Development* **132**, 203-213.
- Takahashi, M., Nomura, T. and Osumi, N. (2008). Transferring genes into cultured mammalian embryos by electroporation. *Dev. Growth Differ.* **50**, 485-497.
- Tanaka, Y., Hayashi, M., Kubota, Y., Nagai, H., Sheng, G., Nishikawa, S. and Samokhvalov, I. M. (2012). Early ontogenic origin of the hematopoietic stem cell lineage. *Proc. Natl. Acad. Sci. USA* **109**, 4515-4520.
- Taoudi, S., Gonneau, C., Moore, K., Sheridan, J. M., Blackburn, C. C., Taylor, E. and Medvinsky, A. (2008). Extensive hematopoietic stem cell generation in the AGM region via maturation of VE-cadherin+CD45+ pre-definitive HSCs. *Cell Stem Cell* **3**, 99-108.
- Tober, J., Koniski, A., McGrath, K. E., Vemishetti, R., Emerson, R., de Mesy-Bentley, K. K., Waugh, R. and Palis, J. (2007). The megakaryocyte lineage originates from hemangioblast precursors and is an integral component both of primitive and of definitive hematopoiesis. *Blood* **109**, 1433-1441.
- Wang, Q., Stacy, T., Binder, M., Marín-Padilla, M., Sharpe, A. H. and Speck, N. A. (1996). Disruption of the Cbfa2 gene causes necrosis and hemorrhaging in the central nervous system and blocks definitive hematopoiesis. *Proc. Natl. Acad. Sci. USA* **93**, 3444-3449.
- Yokomizo, T. and Dzierzak, E. (2010). Three-dimensional cartography of hematopoietic clusters in the vasculature of whole mouse embryos. *Development* **137**, 3651-3661.
- Yokomizo, T., Yamada-Inagawa, T., Yzaguirre, A. D., Chen, M. J., Speck, N. A. and Dzierzak, E. (2012). Whole-mount three-dimensional imaging of internally localized immunostained cells within mouse embryos. *Nat. Protoc.* **7**, 421-431.
- Yoshimoto, M., Montecino-Rodriguez, E., Ferkowicz, M. J., Porayette, P., Shelley, W. C., Conway, S. J., Dorshkind, K. and Yoder, M. C. (2011). Embryonic day 9 yolk sac and intra-embryonic hemogenic endothelium independently generate a B-1 and marginal zone progenitor lacking B-2 potential. *Proc. Natl. Acad. Sci. USA* **108**, 1468-1473.
- Zovein, A. C., Hofmann, J. J., Lynch, M., French, W. J., Turlo, K. A., Yang, Y., Becker, M. S., Zanetta, L., Dejana, E., Gasson, J. C. et al. (2008). Fate tracing reveals the endothelial origin of hematopoietic stem cells. *Cell Stem Cell* **3**, 625-636.

Table S1. Number of embryos analyzed at each age for data displayed in Fig. 2.

Tissue	Genotype	Number of embryos of each age [somite pairs or embryonic age (E)]										
		6-17	18-25	26-30	31-35	36-40	41-45	46-50	51-55	56-60	E13.5	E14.5
Yolk sac	f/f, f/+	13	13	16	16	7	10	11	3			
	f/+; Cre	6	3	4	4	3	3	2	2			
	f/f; Cre	9	3	5	6	6	8	9	3			
Fetal liver	f/f, f/+						12	12	3	11	2	5
	f/+; Cre						1	3	0	5	3	0
	f/f; Cre						4	7	1	11	1	4
AGM+U+V	f/f, f/+		10	13	17	8	15	13				
	f/+; Cre		2	3	2	4	2	2				
	f/f; Cre		3	3	3	4	8	8				

f/f = *Runx1*^{ff}. f/+ = *Runx1*^{f/+}. f/+; Cre = *Runx1*^{f/+}; *Actb-Cre*^{ERT}. f/f; Cre = *Runx1*^{ff}; *Actb-Cre*^{ERT}

Table S2. Number of colonies genotyped at each age for data displayed in Fig. 2.

Tissue	Genotype	Number of colonies analyzed at each age [somite pairs or embryonic age (E)]										
		6-17	18-25	26-30	31-35	36-40	41-45	46-50	51-55	56-60	E13.5	E14.5
Yolk sac	f/+; Cre	99	129	21	64	0	19	50	14			
	f/f; Cre	100	49	92	78	136	105	117	53			
Fetal liver	f/+; Cre						23	65	0	120	98	0
	f/f; Cre						84	111	30	256	64	92
AGM+U+V	f/+; Cre		2	9	55	7	10	54				
	f/f; Cre		8	10	42	37	149	83				

f/+; Cre = *Runx1*^{f/+}; *Actb-Cre*^{ERT}. f/f; Cre = *Runx1*^{f/f}; *Actb-Cre*^{ERT}

Table S3. Number of embryos analyzed at each age for data displayed in Fig. 3.

Tissue	Genotype	Number of embryos of each age (somite pairs)			
		17-23	24-28	29-35	41-50
Yolk sac	f/+, f/f, +/+	9	5	13	6
	f/+; Cre	9	5	2	2
	f/f; Cre	4	4	9	10
Fetal liver	f/+, f/f, +/+				
	f/+; Cre	-	-	-	
	f/f; Cre	-	-	-	
AGM+U+V	f/+, f/f, +/+	7	5	13	6
	f/+; Cre	4	5	2	2
	f/f; Cre	3	4	9	10

f/f = *Runx1^{ff}*. f/+ = *Runx1^{ff+}*. f/+; Cre = *Runx1^{ff+}; VEC-Cre^{ERT}*. f/f; Cre = *Runx1^{ff}; VEC-Cre^{ERT}*

Table S4. Number of colonies genotyped at each age for data displayed in Fig. 3.

Tissue	Genotype	Number of colonies analyzed at each age (in somite pairs)			
		17-23	24-28	29-35	41-50
Yolk sac	f/+; Cre	128	47	48	43
	f/f; Cre	25	69	188	145
AGM+U+V	f/+; Cre	4	27	47	48
	f/f; Cre	7	56	191	159
Fetal liver	f/+; Cre	-	-	-	45
	f/f; Cre	-	-	-	179

f/f = *Runx1*^{f/f}. f/+ = *Runx1*^{f/+}. f/+; Cre = *Runx1*^{f/+}; *VEC-Cre*^{ERT}. f/f; Cre = *Runx1*^{f/f}; *VEC-Cre*^{ERT}